Taylor & Francis
Taylor & Francis Group

Artificial Cells, Nanomedicine, and Biotechnology

An International Journal

ISSN: 2169-1401 (Print) 2169-141X (Online) Journal homepage: https://www.tandfonline.com/loi/ianb20

Using CuO nanoparticles and hyperthermia in radiotherapy of MCF-7 cell line: synergistic effect in cancer therapy

Hadi Esmaeili Govarchin Ghaleh, Leila Zarei, Bahman Mansori Motlagh & Nasrollah Jabbari

To cite this article: Hadi Esmaeili Govarchin Ghaleh, Leila Zarei, Bahman Mansori Motlagh & Nasrollah Jabbari (2019) Using CuO nanoparticles and hyperthermia in radiotherapy of MCF-7 cell line: synergistic effect in cancer therapy, Artificial Cells, Nanomedicine, and Biotechnology, 47:1, 1396-1403, DOI: 10.1080/21691401.2019.1600529

To link to this article: https://doi.org/10.1080/21691401.2019.1600529

Published online: 09 Apr 2019.

ARTIFICIAL CELLS, NANOMEDICINE, AND BIOTECHNOLOGY
2019, VOL. 47, NO. 1, 1396–1403
https://doi.org/10.1080/21691401.2019.1600529

Using CuO nanoparticles and hyperthermia in radiotherapy of MCF-7 cell line: synergistic effect in cancer therapy

Hadi Esmaeili Govarchin Ghaleh[a], Leila Zarei[b], Bahman Mansori Motlagh[b] and Nasrollah Jabbari[b]

[a]Applied Virology Research Center, Baqiyatallah University of Medical Sciences, Tehran, Iran; [b]Solid Tumor Research Center, Urmia University of Medical Sciences, Urmia, Iran

ABSTRACT

The aim of this paper was examining the combined impacts of CuO nanoparticles (CuO NPs), hyperthermia (H), and irradiation (R) on an increment of MCF-7 cells. The MTT assay was employed to assess the antiproliferative effects of CuO NPs (25, 50, and 100 μg/ml), hyperthermia (41 °C for 1 h), and irradiation (200 cGy). Moreover, the perniciousness was estimated through the survival capability of cells, and apoptosis, ROS production, and levels of caspase-3, -8 and -9 proteins were determined. A significant ($p < .01$) decrease in proliferation index (0.124 ± 0.021), a significant ($p < .01$) increase in apoptosis (42% ± 1.54) of MCF7 cells, a significant ($p < .03$) increase in ROS formation (32.16 ± 1.9) and a significant ($p < .01$) increase in LDH release (33.28 ± 1.56) were recorded in the adjacency of MCF-7 cells by a combination of CuO NPs (100 μg/ml) and R + H compared to control and other treatments. The activities of caspase-3 (0.33 ± 0.014) and caspase-9 (0.389 ± 0.019) also increased significantly ($p < .05$). However, caspase-8 showed no significant changes in its activity ($p = .065$). Based on these observations, a combination of CuO NPs, hyperthermia, and irradiation could suppress the growth of MCF-7 cells and evoke cell apoptosis via mitochondrial membrane potential.

ARTICLE HISTORY
Received 11 January 2019
Revised 18 March 2019
Accepted 19 March 2019

KEYWORDS
CuO nanoparticles; hyperthermia; radiation; MCF-7 cells

Introduction

Cancer is nowadays the foremost cause of mortality among threats to mankind, which calls for immediate action and planning. As one of the most widespread types of cancer in female is breast cancer, it is presently cured with various therapies including surgery, radiotherapy, chemotherapy and hormone treatment [1]. A major tumour therapy is radiotherapy that applies ionizing radiation to eradicate cancerous cells [2]. However, the tumour should be delivered with a high radiation dose, which cannot be increased practically in some cases owing to the presence of some functional and healthy tissues hindering the efficacy of this treatment [3]. A number of studies have tried to overcome this problem through the development of new treatments by combining radiation with chemical or thermal agents and improving treatment programs of breast cancer therapy [4]. Among adjunctive treatments are radiosensitizers that render tumour cells more sensitive to radiation [5]. Such substances as nanoparticles and hyperthermia are applied to improve the radiosensitivity of tumoral cells or lessen that of healthy cells [6].

Today, a rapidly growing field of nanotechnology includes the application of nanoparticles to cancer diagnosis and therapy [7–10]. According to a large number of reports, CuO NPs can selectively induce cytotoxicity and DNA damage in the human lung epithelial cell line, namely A549 and K562 [11]. A lower market price than silver and gold, antibacterial effects (against both Gram-negative and Gram-positive microorganisms), and a high sensitivity against microorganisms and/or tumoral cells, even in low concentrations, are the features that distinguish CuO NPs from other anti-cancer NPs [12].

Hyperthermia can potentially raise cytotoxicity within the tumour body without increasing the normal tissue toxicity [13]. The multifunctionality of hyperthermia has been demonstrated in radiosensitization and the higher sensitivity of cancer cells to radiation resulting from the presence of a defensive system in normal cells against heat, whereas cancer cells lack such a system [14]. Through heating to few degrees above physiological temperatures (>37 °C), cancer cells are killed by hyperthermia [15]. Significant cellular responses as a result of hyperthermic points above the uppermost growth temperature include changes in cytoplasmic membrane stability, configuration, potential, hydrogen power, cellular catabolism and anabolism, cytoskeleton and the nuclear matrix [16], generation of macromolecular cellular signaling pathway, heat shock proteins production, transcription factor expression, and changes in the synthesis rate of DNA and RNA [17].

Promoting the remedial efficiency of radiotherapy and anticancer drugs and diminishing their adverse effects with

CONTACT Nasrollah Jabbari njabbarimp@gmail.com Professor of Medical Physics, Solid Tumor Research Center, Department of Medical Physics and Imaging, Urmia University of Medical Sciences, Urmia 571478334, Iran

the aim of improving the quality of life of cancerous patients have been a predominant challenge in cancer therapy hitherto [18]. Chemo drugs in treated cancerous cells kill fast-growing cells. However, because these drugs travel throughout the body, they can affect also normal, healthy cells that are fast growing. One way to overcome this problem is to employ combined treatments including the use of targeted nanoparticles or other multi-agents with radiation and hyperthermia to deliver both chemotherapeutics [19]. Cancerous cells and tissues might be effectively supplied and targeted specifically with gene therapeutics to surmount drug resistance and inhibit the tumour growth [20].

Existing reports indicated that hyperthermia with nanoradiotherapy had an interactive effect corresponding to that of doxorubicin as an anti-cancer drug [21]. Kumar et al. (2017) revealed that temperature changes in the synthesis of cubic HfO_2 nanostructures affected their cytotoxicity on MCF-7 cells [9]. According to Chen et al., the use of selenium combined with radiotherapy on MCF-7 cell line had demonstrated that selenium NPs as an adjuvant could sensitize cancer cells to the toxic impacts of irradiation, resulting in declined damage to normal tissues nearby [22]. In addition, George et al. revealed that Rubus-conjugated Ag NPs induced cell death in MCF-7 cells through the mitochondrial-mediated intrinsic apoptosis pathway [10].

The researchers have proven that combined therapy with NPs, radiation, and hyperthermia enabled the optimization of hyperthermia length and radiation dosage in order to maximize tumour cell death while minimizing cell death in the surrounding tissue. This investigation sought to examine the impacts of radiotherapy, hyperthermia, and CuO NPs alone and in combination on the viability of breast carcinoma (MCF-7) cell lines. Assessments were performed using MTT, apoptosis evaluation via fluorescence microscopy, and caspase assay kit.

Materials and methods

Cell culture and experimental design

The National Cell Bank (Pasteur Institute, Iran) supplied the human MCF-7 breast cancer cells, which were then cultured in RPMI 1640 medium (Sigma, St Louis, MO, USA) containing 10% fetal bovine serum (FBS; Invitrogen), streptomycin (100 mg/ml), and penicillin G (100 units/ml) (Sigma, St Louis, MO, USA). Next, the cells were incubated (37 °C) in a humidified ambiance holding 5% CO2. Thereafter, the cells were divided into 19 groups; Group 1: negative control (NC), Group 2: Radiation (R), Group 3: hyperthermia (H), Group 4: radiation + hyperthermia (R + H), Groups 5, 6, and 7: CuO nanoparticle of 25, 50 and 100 μg/ml (NP 1, NP2 and NP3, respectively), Groups 8, 9 and 10: CuO nanoparticle 25, 50 and 100 μg/ml (NP 1, NP2 and NP3, respectively) + radiation (R), Groups 11, 12 and 13: CuO nanoparticle 25, 50 and 100 μg/ml (NP 1, NP2 and NP3, respectively) + hyperthermia (H), Groups 14, 15 and 16: CuO nanoparticle 25, 50 and 100 μg/ml (NP 1, NP2 and NP3, respectively) + radiation (R) + hyperthermia (R + H), and Groups 17, 18 and 19: positive controls (PC1, PC2 and PC3) using doxorubicin at concentrations of 200, 400, and 800 nM, respectively.

Identification and formulation of CuO NPs

Transmission electron microscopy (TEM) image and the CuO NPs characteristics including X-ray diffraction pattern by Iranian Nanomaterials Pioneers Company, NANOSANY (Mashhad, Iran) have been illustrated in Figure 1. Sorted concentrations of CuO NPs were prepared by initial sterilization of CuO nanopowder with UV irradiation (6-W UV-C lamp with a length of 30 cm placed 5 cm above the samples) emitted from the lamp at an uppermost wavelength (254 nm). The desired light intensity (1.8 W/m2) was measured using a radiometer (Hagner ECL-X) at 200–400 nm. Thereafter, a suspension of CuO NPs in RPMI-1640 was diluted to suitable concentrations. Selection of 25, 50 and 100 μg/ml at dosage range of CuO NPs was based on preliminary dose–response experiments (data not shown) and calculated LD50 and IC50. A sonicator bath (UP200H/Hielscher, Germany) was employed in the second stage to sonicate CuO NPs dilutions (40 W and 24 kHz frequency) at room temperature for 15 min, after which the cells were subjected to treatments.

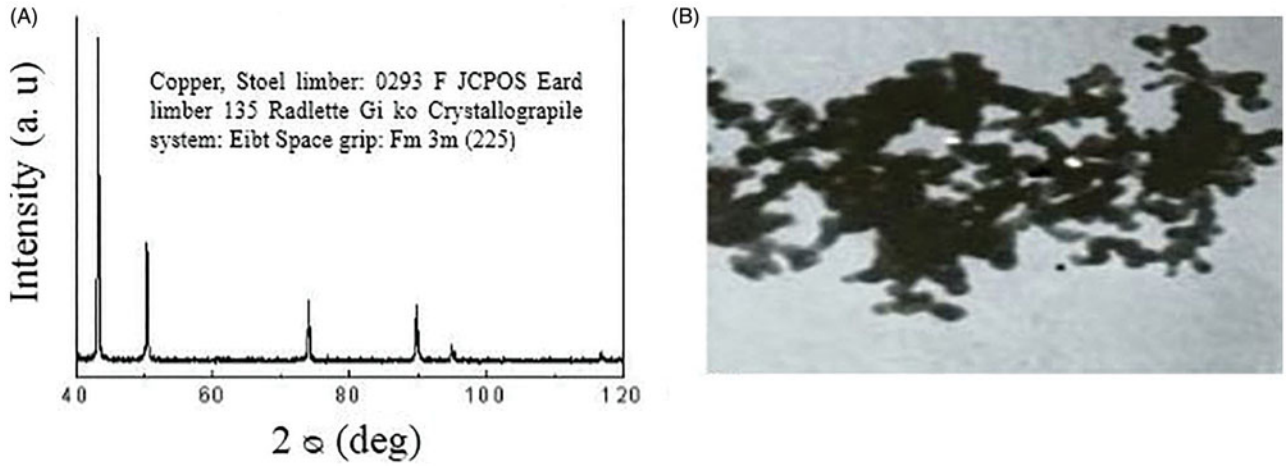

Figure 1. X-ray diffractogram (A) and transmission electron microscopy (TEM) image of copper oxide nanoparticles (B).

Measurement of CuO NP uptake

A study conducted by Shafagh et al. (2015) revealed that CuO NPs had the most cytotoxicity activity on cancer cells but not on normal peripheral blood mononuclear cell (PBMCs). Hence, experiments were not repeated on normal cells [23]. In the trial initial phase, a suspension of 1×10^6 MCF-7 cells was made in RPMI-1640 and incubated separately (at 37 °C) in 5% CO_2 in a range of CuO NPs concentrations (25, 50 and 100 μg/ml) for 24 h. To discard non-uptake nanoparticles, the second-phase treated cells were rinsed thrice by phosphate buffered saline (PBS). Subsequently, 3% HCl (0.3 ml) in concentrated HNO3 was used to digest the cells at room temperature overnight, followed by the addition of indium at 5 μl of 5-ppm (as the internal standard), and 5 ml of matrix solution (2% HCl and 2% HNO3). CuO NPs contents in individual samples were determined using spectrophotometry at 280 nm with an atomic absorption device (Model 603, Perkins Elmer, Waltham, MA), and comparisons were made with a standard curve [24].

ROS production assay

Dichlorodihydrofluorescein diacetate (DCF-DA, 2.5 μM; Invitrogen, St Louis, MO, USA) was used to measure ROS generation. After passive penetration of DCFH-DA into the cell, it forms dichlorofluorescein (DCF), as a highly fluorescent compound, through reacting with ROS. The detached cells were briefly treated with the multi-agent combination from 24-well plates by 0.05% trypsin/EDTA solution, and 1×10^6 cells/well were transferred to 6-well plates for 24 h. After washing twice with PBS, the cells were stained by 20 μM DCFH-DA within 30 min and incubated in DCFH-DA. The cells were then washed with PBS, and the fluorescence intensities were specified by control. The images of the treated cells were observed under a fluorescence microscope (Olympus CKX 41) with a magnification of 40X [23].

Irradiation and hyperthermic exposure

The treatment of MCF-7 cells with irradiation and hyperthermia included initial seeding of 1×10^6 cells/well in RPMI-1640 (200 μl) alone and with CuO NPs (25, 50 and 100 μg/ml) in individual wells of 24-well plates. Precultured cells were then prepared through nightlong incubation (37 °C). Upon changing the culture medium in all experiments, the cell-seeded plates were relocated in the cell culture incubator (SB-14012, Germany) at 41 °C for 1 h (hyperthermia process). Following hyperthermia, in the irradiated groups, the cells plate was exposed with 200 cGy of a cobalt-60 γ-ray source (Theratron Phoenix, Theratronics, Inc., Ottawa, Canada) with an approximate dose rate of 34 cGy/min (source to skin distance [SSD] of 79.5 cm) at room temperature. In the end, the cells in all treated groups with multi-agent combination underwent a one-day incubation (37 °C) in a 5% CO_2 ambiance, prior to cell sampling for evaluation [21,25,26].

Cell viability

As reported by Jabbari et al. [21], MTT assay for the viability of MCF-7 cells was examined against multi-agent combination treatment groups. To summarize, after treating the isolated cells with a multi-agent combination from 24-well plates by 0.05% trypsin/EDTA solution, the cells were transferred to 1×10^6 cells/well in 96-well plates for 48 h. MTT (20 μl, 5 mg/ml) was distributed to each well, 4 h prior to the termination of 48 h, after which the plate was incubated (37 °C) for 4 h to develop a purple-coloured formazan product. Following the addition of DMSO (dimethyl sulfoxide, 100 μl) to the plate, it was incubated at 37 °C for dissolution of purple crystals in 10 min. An ELISA plate reader (Dana 3200, Iran) measured the optical density (OD) of individual wells at a wavelength of 492 nm. Calculation of the cell viability was based on the following procedure.

$$\text{Cell viability } (\%) = \frac{\text{Optical density value of test}}{\text{Optical density value of control}} \times 100$$

The half maximal inhibitory concentration (IC50) is the drug concentration causing 50% inhibition of the desired activity and LD50 is the concentration causing 50% cell death (LD = lethal dose). In the current study, IC50 and LD50 were the same, because the means of activity was the inhibition of biological activity of cells (cell death).

The IC50 and lowest lethal dose for our cytotoxic study were determined by linear regression and based on the following procedure (the values of Y are in the range of 0–1) [27].

$$\text{A) } Y = aX + b \qquad \text{B) } IC50 = (0.5 - b)/a$$

Evaluation of MCF-7 apoptosis

Acridine orange and propidium iodide were used to examine the percentage of MCF-7 cells against multi-agent combination treatment groups as defined by Jabbari et al. [21]. To sum up, the isolated cells were treated by multi-agent combinations from 24-well plates using 0.05% trypsin/EDTA solution. The group-specific cell suspension was rinsed with PBS. Next, a fluorescent dye (10 μl) consisting of acridine orange (10 μg/ml) and Propidium Iodide (10 μg/ml) with equal volumes was decanted into the cellular pellet. Under fluorescent microscopy (Olympus CKX41), estimation of apoptotic cells (%) was performed in an upgraded Neubauer rhodium hemocytometer.

Lactate dehydrogenase assay (LDH)

Lactate dehydrogenase (LDH) is an enzyme widely present in cytosol that converts lactate into pyruvate. When plasma membrane integrity is ruptured, LDH leaks into culture media and its extracellular level is increased. Cytotoxicity was assessed using LDH Kit (Abcam, ab65393). This assay measures the release of cytoplasm enzyme lactate dehydrogenase (LDH) by damaged cells. Cells cultured in 96 plates were treated with multi-agent. After 48 h of treatment, culture

supernatant was collected and incubated with reaction mixture. The LDH catalyzed conversion resulted in the reduction of the tetrazolium salt to Formosan, which could be read at 490 nm absorbance [28].

Examination of caspase-3, -8 and -9 formation

Caspase-3, -8 and -9 protein concentrations were appraised by colourimetric assay kits (Sigma-Aldrich, St. Louis, MO) after MCF-7 cells had been treated with multi-agent combination treatment groups as described by the manufacturer's guidelines and Jabari et al. [21].

Statistical analysis

Data were analyzed with one-way ANOVA and presented as mean ± standard deviation (SD) to compare the experimental groups. Once significant differences were detected using ANOVA, mean values between different groups were compared by Tukey's multiple post-hoc test. Significant differences between the groups were considered when $p < .05$.

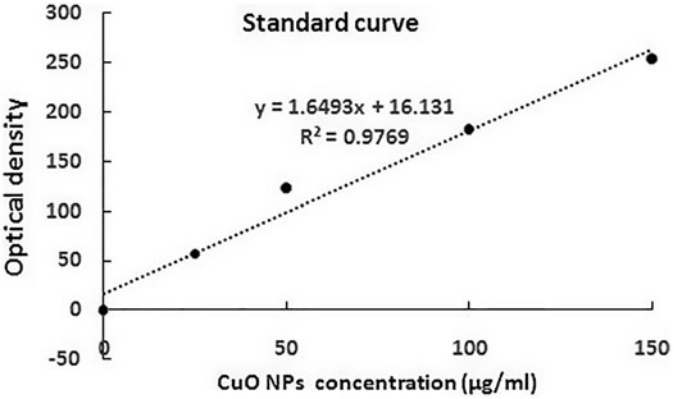

Figure 2. Standard curve for cellular uptake of copper oxide nanoparticles (CuO NPs) into the MCF-7 cells in concentrations of 25, 50 and 100 µg/mL.

Results

Physicochemical characterization of CuO nanoparticles

The illustrations of TEM from CuO NPs demonstrating a majority of the particles in a spherical shape and with smooth surfaces have been displayed in Figure 1. An average of 20 nm was calculated for the TEM diameter of CuO NPs.

Measuring in vitro cellular uptake of nanoparticles

Based on the standard curve in Figure 2, CuO NPs at concentrations of 25, 50 and 100 µg/mL were drawn into the MCF-7 cells at amounts of 5.37, 20.53 and 50.85 µg/mL, respectively.

Cell cytotoxicity (MTT assay) and viability/apoptosis results

As presented in Table 1, the *in vitro* cytotoxicity of CuO NPs and multi-agent combination treatment groups against breast cancer cell lines MCF-7 was performed using MTT, apoptosis and LDH assays. The results were compared to the standard Doxorubicin and negative control group. The highest value was 100-µg/mL NPs + R + H in cytotoxicity groups in comparison with the control and other groups (Figure 3). Furthermore, the NP1, NP2 and NP3 treatments revealed significantly larger cell cytotoxicity with rising concentrations of CuO NPs from 25 to 100 µg/mL. The IC50 and lowest lethal dose values of the CuO NPs against MCF-7 cell lines were 184.38 and 6.25 µg/ml, respectively (Figure 4). The outcomes of cytotoxicity disclosed further effectiveness of NPs mixed with R + H, and the use of NPs combined with H only was not more operative than R or R + H. Table 1 indicates that

Table 1. Mean ± standard deviations (SD) of investigated parameters in the groups under study.

	Mean ± SD of Variables			
Groups	MTT assay (absorbance)	Apoptosis (%)	ROS (DCF-Positive cell)	LDH assay (%)
NC	0.297 ± 0.02^{a}	17.75 ± 2.43^{a}	7.2 ± 2.03^{a}	9.03 ± 1.2^{a}
R	0.226 ± 0.014^{d}	25 ± 2.8^{d}	15.01 ± 2.11^{c}	16.28 ± 1.27^{b}
H	0.274 ± 0.01^{ac}	20.36 ± 3.4^{a}	10.23 ± 1.02^{a}	11.64 ± 1.32^{ac}
R + H	0.2 ± 0.006^{d}	26 ± 3^{d}	16.41 ± 1.6^{c}	17.28 ± 1.03^{b}
NP1	0.253 ± 0.011^{c}	23.6 ± 1.45^{d}	13.56 ± 2.13^{c}	14.88 ± 2.12^{bc}
NP2	0.205 ± 0.021^{d}	28.56 ± 2.14^{e}	18.2 ± 2.14^{d}	19.84 ± 2.03^{b}
NP3	0.185 ± 0.014^{d}	30.2 ± 2.36^{e}	20.14 ± 1.03^{d}	21.48 ± 1.23^{bd}
NP1 + R	0.201 ± 0.26^{d}	28.36 ± 1.23^{e}	18.45 ± 2.03^{d}	19.64 ± 1.02^{b}
NP2 + R	0.186 ± 0.018^{d}	31.26 ± 2.14^{eb}	21.23 ± 1.4^{d}	22.54 ± 1.14^{bd}
NP3 + R	0.136 ± 0.01^{b}	38 ± 1.8^{c}	28.41 ± 2.14^{b}	29.28 ± 1.85^{e}
NP1 + H	0.224 ± 0.023^{d}	24.36 ± 1.5^{d}	14.16 ± 1.63^{c}	15.64 ± 1.26^{abc}
NP2 + H	0.197 ± 0.024^{d}	28.36 ± 1.5^{e}	18.45 ± 2.12^{d}	19.64 ± 2.5^{abc}
NP3 + H	0.185 ± 0.017^{d}	28.42 ± 2.13^{c}	21.45 ± 1.8^{de}	19.7 ± 1.46^{abc}
NP1 + R + H	0.184 ± 0.015^{d}	28.26 ± 2.9^{ed}	22.36 ± 3.01^{de}	19.54 ± 1.26^{abc}
NP2 + R + H	0.142 ± 0.012^{be}	35.62 ± 3.06^{ce}	25.14 ± 2.14^{de}	26.9 ± 1.41^{d}
NP3 + R + H	0.124 ± 0.021^{be}	42 ± 1.54^{c}	32.16 ± 1.9^{b}	33.28 ± 1.56^{e}
PC1	0.163 ± 0.008^{b}	33.50 ± 1.25^{b}	23.11 ± 3.8^{b}	24.78 ± 1.36^{d}
PC2	0.151 ± 0.011^{b}	38.75 ± 2.36^{c}	28.21 ± 3.6^{b}	30.03 ± 1.27^{e}
PC3	0.14 ± 0.029^{b}	41.50 ± 3.51^{c}	30.26 ± 3.56^{b}	32.78 ± 1.17^{e}
p-Values	$p < .05$	$p < .05$	$p < .05$	$p < .05$

The abbreviations are provided in experiment design of section "Materials and methods".
Doxorobicin was considered as positive control (PC); NPs: nano particles; R: radiation; H: hyperthermia. Significant statistical differences between groups in each index are indicated by the different superscript letter ($p < 0.05$).

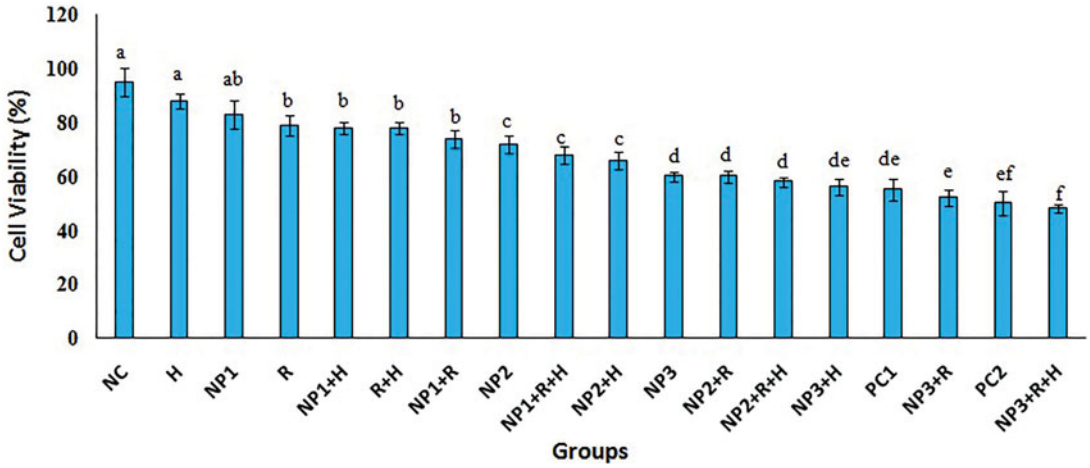

Figure 3. Effects of radiation (R), hyperthermia (H), copper oxid nanoparticle (CuO NPs) and doxorubicin, as positive control (PC), on the cell viability of MCF-7 cells in the studied groups. The abbreviations are provided in experiment design of section "Materials and methods". The values were normalized to those of negative control group. Significant statistical differences between groups in each index are indicated by the different superscript letter ($p < .05$).

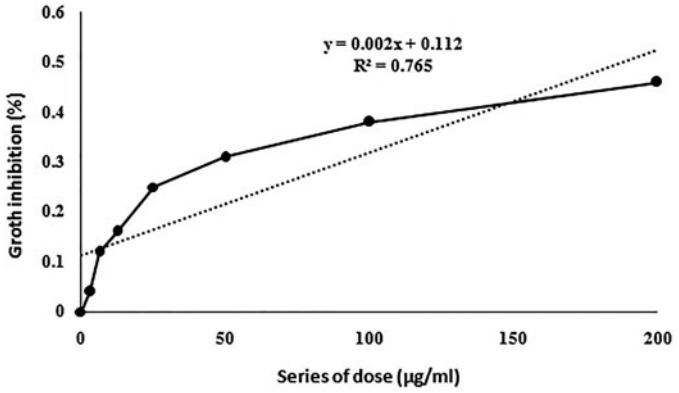

Figure 4. The effect of CuO NPs on MCF-7 cell line. The IC50 was calculated based on the linear regression.

the effect of cytomorphological changes in CuO NPs on MCF-7 cell lines at various concentrations (25, 50 and 100 μg/mL) includes intracellular suicide program having such morphological changes as cell shrinkage, oxidative stress, coiling and biochemical response resulting in apoptosis. The observations obviously demonstrate enlarged apoptosis rate (viability) of MCF-7 cell lines with ascending concentrations of CuO NPs plus radiation and hyperthermia as seen in cytotoxicity results (Table 1). The uppermost concentration (100 μg/mL + R + H) yielded maximum inhibition of breast cancer's cell lines, with H group showing the least impact on the viability of MCF-7 cells. Acridine orange/propidium iodide was used to evaluate the survival of MCF-7 cells. The cell lines were categorized based on their colour and chromatin morphology. As shown in Figure 5, the green cells with diffused chromatin are viable, the cells with condensed chromatin are apoptotic and the red cells with no condensed chromatin are necrotic.

ROS production

Compared to the negative control group, ROS production increased significantly in the treated groups along with the dose-dependent behaviour of NPs ($p < .05$; Table 1). The highest and lowest amounts of ROS were generated in NP3 + R + H and H groups, respectively. Although, ROS creation was affected by the concentration of CuO NPs rising from 25 to 100 μg/mL however the R + H addition gave rise to the formation of ROS.

LDH assay

As presented in Table 1, LDH activity was measured to observe the effect of CuO NPs and multi-agents on membrane integrity by treating MCF-7 cells for 48 h. The results proved that the influence of CuO NPs on the cell membrane integrity of MCF-7 cells responded in a dose-dependent manner and increased through adding radiation and hyperthermia. The 100 μg/mL + R + H group yielded maximum LDH release of breast cancer`s cell lines.

Caspase assay

No significant increase was observed in caspase-8 levels of the cells subjected to 24 h incubation in CuO NPs (25, 50 and 100 μg), radiation and hyperthermia ($p < .05$). However, levels of Caspase-9 and -3 in all groups elevated significantly after 24 h of incubation, but H group showed no significant changes with the NC group ($p < .05$) (Table 2).

Discussion

The current study mainly aimed to investigate the impacts of CuO NPs and hyperthermia as factors with a strong potential in raising cytotoxicity of radiotherapy on breast carcinoma (MCF-7) cell lines. MTT assay was applied to evaluate the cytotoxicity of combined multi-agent (CuO NPs + R + H). According to the findings, cytotoxic effects on MCF-7 cell line were detected in all treated groups, with the highest and lowest cytotoxic effects recorded for 100 μg/ml + R + H and H groups, respectively, on MCF-7 cell line. Moreover, cytotoxic effects rose with increasing concentration of NPs and addition of R and H. MCF-7 cell viability after treatment with combined multi-agents showed the lowest and highest cell

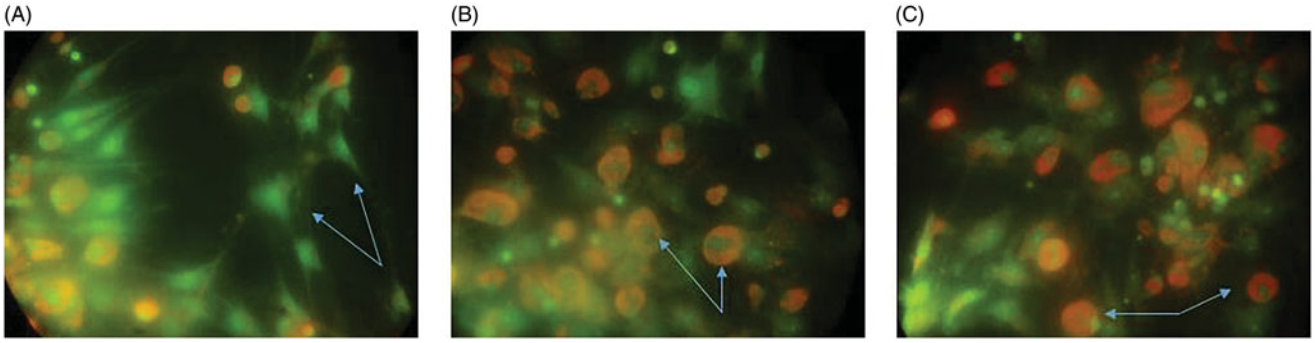

Figure 5. The assessment of MCF-7 apoptosis by propidium iodide/acridine orange staining. The green cells with diffused chromatin are viable (A), the cells with condensed chromatin are apoptotic (B) and the red cells with no condensed chromatin are necrotic (C).

Table 2. Descriptive statistics (mean ± standard deviations (SD)) of investigated of caspase-3, -8, and -9 activities in the groups under study.

	Mean ± SD of Variables		
Groups	Caspase-3 activity	Caspase-8 activity	Caspase-9 activity
NC	0.201 ± 0.01^{a}	0.294 ± 0.044^{a}	0.108 ± 0.026^{a}
R	0.24 ± 0.016^{d}	0.3 ± 0.017	0.16 ± 0.025^{c}
H	0.201 ± 0.026^{a}	0.251 ± 0.027^{a}	0.142 ± 0.011^{da}
R + H	0.265 ± 0.02^{d}	0.302 ± 0.01^{a}	0.189 ± 0.014^{d}
NP1	0.266 ± 0.017^{d}	0.319 ± 0.019^{a}	0.16 ± 0.032^{d}
NP2	0.275 ± 0.014^{d}	0.325 ± 0.016^{a}	0.201 ± 0.025^{d}
NP3	0.298 ± 0.017^{de}	0.362 ± 0.033^{a}	0.235 ± 0.036^{de}
NP1 + R	0.303 ± 0.02^{e}	0.341 ± 0.02^{a}	0.256 ± 0.014^{e}
NP2 + R	0.3 ± 0.017^{e}	0.332 ± 0.036^{a}	0.254 ± 0.025^{e}
NP3 + R	0.285 ± 0.02^{e}	0.330 ± 0.024^{a}	0.295 ± 0.021^{e}
NP1 + H	0.319 ± 0.021^{e}	0.356 ± 0.018^{a}	0.22 ± 0.02^{e}
NP2 + H	0.274 ± 0.025^{e}	0.330 ± 0.026^{a}	0.22 ± 0.014^{d}
NP3 + H	0.284 ± 0.02^{e}	0.323 ± 0.016^{a}	0.256 ± 0.016^{d}
NP1 + R + H	0.3 ± 0.014^{e}	0.342 ± 0.036^{a}	0.345 ± 0.02^{de}
NP2 + R + H	0.325 ± 0.026^{e}	0.340 ± 0.039^{a}	0.362 ± 0.014^{b}
NP3 + R + H	0.33 ± 0.014^{e}	0.325 ± 0.016^{a}	0.389 ± 0.019^{b}
PC1	0.357 ± 0.014^{b}	0.328 ± 0.011^{a}	0.324 ± 0.033^{b}
PC2	0.371 ± 0.026^{b}	0.359 ± 0.08^{a}	0.389 ± 0.012^{c}
PC3	0.446 ± 0.033^{c}	0.362 ± 0.04^{a}	0.423 ± 0.047^{c}
p-Values	$p < .05$	$p = .065$	$p < .05$

The abbreviations are provided in experiment design of section "Materials and methods".

Doxorobicin was considered as positive control (PC); NPs: nano particles; R: radiation; H: hyperthermia. Significant statistical differences between groups in each index are indicated by the different superscript letter ($p < .05$).

viability in 100 μg/ml + R + H and H groups, respectively. Having a dose-dependent behaviour in the properties of combined multi-agent, an outcome confirmed the results of MTT.

CuO NPs have been shown to have a selective cytotoxic effect on k562 cell line in a dose-dependent manner. In addition, the viability of K562 cells declined significantly to 57% at 10 μg/ml [23]. As reported by Azizi et al. [25], albumin coated copper nanoparticle exerted a highly toxic effect on human breast cancer cells (MDA-MB 231) compared to normal cells. Moreover, the apoptosis induction pathway was associated with increased mitochondrial membrane potential and activations of caspase-3 and -9. The authors demonstrated that this combined multi-agent was a potential candidate as a chemotherapeutic agent for invasive breast cancer cells.

In the therapeutic hyperthermia procedure, tissues are heated to a higher temperature, normally in the range of 41–45 °C [26]. This process has been combined with radiotherapy and/or chemotherapy and investigated for long years, yielding considerable success in curing advanced and recurrent cancers [29,30].

Apoptosis is induced by cytotoxic agents through the initiation of death signalling pathways in vulnerable target cells [31]. Death receptor systems after activation cause the infraction of mitochondrial function and activated of caspases cleavage that all it involved in activation of apoptosis by anticancer agents [32]. Consequently, the cell death route might ensue in several positions; yet, the exact molecular mechanisms are not fully characterized for every particular drug and specifically intended cells [33]. During apoptosis, caspases are activated in numerous cells and are known to have a vital contribution to both initiation and accomplishment of apoptosis [34].

Recently, the toxicity of CuO NPs has been shown to be mediated by oxidative stress in various cell lines including A549 cell line, human cardiac microvascular endothelial, kidney and neuronal cells [35]. A study by Wang et al. [36] revealed that cytotoxicity of CuO NPs in HepG2 cells depended on an association between reactive ROS production and gene expression when exposed to CuO NPs. They also observed an apoptotic mode of cell death mediated by the ROS activated mitochondrial pathway, as supported by dropping caspase-8 levels and expression of cleaved caspase-9 proteins [37].

CuO NPs significantly alleviated cell viability in a dose-dependent manner. This is suggested to be caused by oxidative stress as an important agent in the NPs' toxicity mechanisms [38]. In this research, production of caspases 3 and 9 in MCF-7 cells was induced by CuO NPs, radiation and hyperthermia, and all groups of MCF-7 cells presented apoptosis and ROS generation. Morphological changes of radiation and hyperthermia on MCF-7 cells were confirmed by the results of MTT for CuO NPs cytotoxicity. One of the best ways to determine apoptosis is morphological characterization via fluorescence microscopy [39]. The CuO NPs and combined treatment in this research raised the quantity of cells in primary and late phases of apoptosis.

Cytotoxicity, induced by CuO NPs, and multi-agents were assessed by lactate dehydrogenase (LDH) leakage into the culture medium. LDH release, a cytoplasmic enzyme, was the consequence of cell membrane rupture [28]. Cell membrane rupture was defined as the ratio of LDH activity in the supernatant of treated cells to the LDH activity released in the control cells. In this study, the levels of cytosolic enzyme

Lactate Dehydrogenase (LDH) was significantly elevated after 48 h of all treatments in the medium when compared to the control. Moreover, the highest LDH release was in CuO NPs (100 μg/ml) with R + H groups as compared to control. Shaheen et al. revealed that assessments of the GO-ZnO against the MCF-7 Cells, a significant increased the LDH release in a dose-dependent manner [40].

A recent study presented evidence that activated caspase-3 (cleaved caspase-3) was the key for apoptosis induction [41]. Altogether, up-regulation of p53 gave rise to the stimulation of pro-apoptotic members from the Bcl-2. Bax family, for instance, arouses permeabilization of the exterior mitochondrial membrane, which promoted caspase-9 activation by releasing soluble proteins from the intermembrane space into the cytosol [42]. Using caspase kit, alterations were noticed in the production of caspases engaged in the damage response pathway. According to the current study's observations, CuO NPs and combined treatment raised the levels of caspase-3 and -9 while reducing the production of caspase-8. Activated caspase-3 could autocatalytically activate other caspases, which resulted in rapid and irretrievable apoptosis [43]. In a study by Sharifi et al., doxorubicin-induced mitochondrial-dependent apoptosis was induced by down-regulation of Bcl-xL and up-regulation of Bax and caspase-9 expressions. Additionally, Shafagh et al. noticed the mitochondrial-dependent induction of apoptosis by CuO NPs [23,44]. The present results proved that CuO NPs combined with hyperthermia and radiotherapy could induce mitochondrial-dependent apoptosis by down-regulation of caspase-8 and up-regulation of caspase-9 expressions, which corroborated all previous reports.

In conclusion, the observations in the present study revealed the induction of apoptosis mediated by ROS generation in MCF-7 cells CuO NPs using combined radiation and hyperthermia. According to the results of caspase assay, cell apoptosis was induced by CuO NPs via potential of mitochondrial membrane together with elevations and activations of caspase-3 and -9.

Acknowledgements

The authors hereby acknowledge the Research Vice Chancellor (VCR) at Urmia University of Medical Sciences (Urmia, Iran) who approved and supported this project. Special thanks go to the physicians and staff of the Omid Research and Treatment Center (Urmia, Iran) who helped us in the present study.

Disclosure statement

The authors report that they have no conflict of interest. The authors individually accept the responsibility for the content of this article.

References

[1] Naz S, Shahzad H, Ali A, et al. Nanomaterials as nanocarriers: a critical assessment why these are multi-chore vanquisher in breast cancer treatment. Artif Cells Nanomed Biotechnol. 2018;46:899–916.

[2] Zhang X, Liu Z, Lou Z, et al. Radiosensitivity enhancement of Fe_3O_4@Ag nanoparticles on human glioblastoma cells. Artif Cells Nanomed Biotechnol. 2018;3:1–10.

[3] Arya G, Kumari RM, Gupta N, et al. Green synthesis of silver nanoparticles using Prosopis juliflora bark extract: reaction optimization, antimicrobial and catalytic activities. Artif Cells Nanomed Biotechnol. 2018;46:985–993.

[4] Liu Z, Tan H, Zhang X, et al. Enhancement of radiotherapy efficacy by silver nanoparticles in hypoxic glioma cells. Artif Cells Nanomed Biotechnol. 2018;11:1–9.

[5] Huerta S, Gao X, Livingston EH, et al. In vitro and in vivo radiosensitization of colorectal cancer HT-29 cells by the smac mimetic JP-1201. Surgery. 2010;148:346–353.

[6] Wang C, Jiang Y, Li X, et al. Thioglucose-bound gold nanoparticles increase the radiosensitivity of a triple-negative breast cancer cell line (MDA-MB-231). Breast Cancer. 2015;22:413–420.

[7] Badrzadeh F, Rahmati-Yamchi M, Badrzadeh K, et al. Drug delivery and nanodetection in lung cancer. Artif Cells Nanomed Biotechnol. 2016;44:618–634.

[8] Wicki A, Witzigmann D, Balasubramanian V, et al. Nanomedicine in cancer therapy: challenges, opportunities, and clinical applications. J Control Release. 2015;200:138–157.

[9] Kumar N, George BPA, Abrahamse H, et al. A novel approach to low-temperature synthesis of cubic HfO2 nanostructures and their cytotoxicity. Sci Rep. 2017;7:9351.

[10] George PA, Kumar B, Abrahamse N, et al. Apoptotic efficacy of multifaceted biosynthesized silver nanoparticles on human adenocarcinoma cells. Sci Rep. 2018;8:14368.

[11] Aparna Y, Venkateswara Rao K, Srinivasa Subbarao P. Preparation and Characterization of CuO Nanoparticles by Novel Sol-Gel Technique. J Nano-Electron Phys. 2012;4:3005–3008.

[12] Jeronsia JE, Vidhya Raj DJ, Joseph LA, et al. In vitro antibacterial and anticancer activity of copper oxide nanostructures in human breast cancer Michigan Cancer Foundation-7 cells. J Med Sci. 2016;36:145–151.

[13] Dou JP, Zhou QF, Liang P, et al. Advances in nanostructure-mediated hyperthermia in tumor therapies. Curr Drug Metab. 2018;19:85–93.

[14] Ahmed K, Zaidi SF. Treating cancer with heat: hyperthermia as promising strategy to enhance apoptosis. J Pak Med Assoc. 2013;63:504–508.

[15] Lee CT, Mace T, Repasky EA. Hypoxia-driven immunosuppression: a new reason to use thermal therapy in the treatment of cancer? Int J Hyperthermia. 2010;26:232–246.

[16] Muthana M, Multhoff G, Pockley AG. Tumour infiltrating host cells and their significance for hyperthermia. Int J Hyperthermia. 2010;26:247–255.

[17] Cui ZG, Piao JL, Rehman MU, et al. Molecular mechanisms of hyperthermia-induced apoptosis enhanced by withaferin A. Eur J Pharmacol. 2014;723:99–107.

[18] Munaweera I, Shi Y, Koneru B, et al. Chemoradiotherapeutic magnetic nanoparticles for targeted treatment of nonsmall cell lung cancer. Mol Pharmaceutics. 2015;12:3588–3596.

[19] Yoney A, Isikli L. Preoperative chemoradiation in locally advanced rectal cancer: a comparison of bolus 5-fluorouracil/leucovorin and capecitabine. Saudi J Gastroenterol. 2014;20:102–107.

[20] Richard V, Nair MG, Santhosh Kumar TR, et al. Side population cells as prototype of chemoresistant, tumor-initiating cells. Biomed Res Int. 2013;2013:1.

[21] Jabbari N, Zarei L, Esmaeili Govarchin Galeh H, et al. Assessment of synergistic effect of combining hyperthermia with irradiation and calcium carbonate nanoparticles on proliferation of human breast adenocarcinoma cell line (MCF-7 cells). Artif Cells Nanomed Biotechnol. 2018;46:364–372.

[22] Chen F, Zhang XH, Hu XD, et al. The effects of combined selenium nanoparticles and radiation therapy on breast cancer cells in vitro. Artif Cells Nanomed Biotechnol. 2018;46:937–948.

[23] Shafagh M, Rahmani F, Delirezh N. CuO nanoparticles induce cytotoxicity and apoptosis in human K562 cancer cell line via

mitochondrial pathway, through reactive oxygen species and P53. Iran J Basic Med Sci. 2015;18:993–1000.
[24] Choi CHJ, Hao L, Narayan SP, et al. Mechanism for the endocytosis of spherical nucleic acid nanoparticle conjugates. Proc Natl Acad Sci USA. 2013;110:7625–7630.
[25] Azizi M, Ghourchian H, Yazdian F, et al. Cytotoxic effect of albumin coated copper nanoparticle on human breast cancer cells of MDAMB 231. PLoS One. 2017;12:e0188639.
[26] Chatterjee DK, Diagaradjane P, Krishnan S. Nanoparticle-mediated hyperthermia in cancer therapy. Ther Deliv. 2011;2:1001–1014.
[27] Wirz J. Springer protocols and Wiley current protocols. J Med Libr Assoc. 2014;102:304–305.
[28] Alarifi S, Ali D, Alkahtani S, et al. Iron oxide nanoparticles induce oxidative stress, DNA damage, and caspase activation in the human breast cancer cell line. Biol Trace Elem Res. 2014;159:416–424.
[29] Lee H, Park HJ, Park CS, et al. Response of breast cancer cells and cancer stem cells to metformin and hyperthermia alone or combined. PLoS One. 2014;9:e87979.
[30] Ghahremani FH, Sazgarnia A, Bahreyni-Toosi MH, et al. Efficacy of microwave hyperthermia and chemotherapy in the presence of gold nanoparticles: an in vitro study on osteosarcoma. Int J Hyperthermia. 2011;27:625–636.
[31] Colombo R, Moschini M. Role of the combined regimen with local chemotherapy and Mw-induced hyperthermia for non-muscle invasive bladder cancer management. A systematic review. Urologia. 2013;80:112–119.
[32] Zagar TM, Higgins KA, Miles EF, et al. Durable palliation of breast cancer chest wall recurrence with radiation therapy, hyperthermia, and chemotherapy. Radiother Oncol. 2010;97:535–540.
[33] Zhang Z, Wang CH, Du GJ, et al. Genistein induces G2/M cell cycle arrest and apoptosis via ATM/p53-dependent pathway in human colon cancer cells. Int J Oncol. 2013;43:289–296.
[34] Jinesh GG, Kamat AM. Blebbishield emergency program: An apoptotic route to cellular transformation. Cell Death Differ. 2016;23:757–758.
[35] Chang YN, Zhang M, Xia L, et al. The toxic effects and mechanisms of CuO and ZnO nanoparticles. Materials. 2012;5:2850–2871.
[36] Wang S, Liu H, Zhang Y, et al. The effect of CuO NPs on reactive oxygen species and cell cycle gene expression in roots of rice. Environ Toxicol Chem. 2015;34:554–561.
[37] Zhao J, Wang ZY, Liu XY, et al. Distribution of CuO nanoparticles in juvenile carp (*Cyprinus carpio*) and their potential toxicity. J Hazard Mater. 2011;197:304–310.
[38] Fu X. Oxidative stress induced by CuO nanoparticles (CuO NPs) to human hepatocarcinoma (HepG2) cells. Jct. 2015;06:889–895.
[39] Siddiqui MA, Ahamed M, Ahmad J, et al. Nickel oxide nanoparticles induce cytotoxicity, oxidative stress and apoptosis in cultured human cells that is abrogated by the dietary antioxidant curcumin. Food Chem Toxicol. 2012;50:641–647.
[40] Shaheen F, Aziz MH, Fatima M, et al. In vitro cytotoxicity and morphological assessments of GO-ZnO against the MCF-7 cells: determination of singlet oxygen by chemical trapping. Nanomaterials (Basel). 2018;8:539.
[41] Xu J, Li Z, Xu P, et al. Nanosized copper oxide induces apoptosis through oxidative stress in podocytes. Arch Toxicol. 2013;87:1067–1073.
[42] Elkholi R, Renault TT, Serasinghe MN, et al. Putting the pieces together: how is the mitochondrial pathway of apoptosis regulated in cancer and chemotherapy? Cancer Metab. 2014;2:16.
[43] Yu-Min K, Tung-Ying W, Yang-Changm W, et al. Annonacin induces cell cycle-dependent growth arrest and apoptosis in estrogen receptor-α-related pathways in MCF-7 cells. J Ethnopharmacol. 2011;137:1283–1290.
[44] Sharifi S, Barar J, Hejazi MS, et al. Doxorubicin changes Bax/Bcl-xL ratio, caspase-8 and 9 in breast cancer cells. Adv Pharm Bull. 2015;5:351–359.